STATE RESEARCH CENTER OF RUSSIA

INSTITUTE FOR HIGH ENERGY PHYSICS

IHEP 97-42

L.G.Landsberg, V.V.Molchanov

RADIATIVE DECAYS OF HYPERONS

Protvino 1997

UDK 681.3.00.069 M–24

Abstract

Landsberg L.G., Molchanov V.V. Radiative Decays of Hyperons: IHEP Preprint 97-42. – Protvino, 1997. – p. 21, figs. 6, tables 3, refs.: 46.

A possibility to study radiative transitions of the several hyperon resonances in the Coulomb production in the high energy hyperons beams is discussed in the framework of the SELEX experiment at the Tevatron.

Аннотация

Ландсберг Л.Г., Молчанов В.В. Радиационные распады гиперонов: Препринт ИФВЭ 97-42. – Протвино, 1997. – 21 с., 6 рис., 3 табл., библиогр.: 46.

В работе обсуждаются возможности изучения радиационных переходов для ряда гиперонных резонансов в кулоновском рождении в гиперонном пучке высокой энергии в рамках эксперимента SELEX на Теватроне (Фермилаб).

Introduction

In recent years the amount of work on the electromagnetic decays of hadrons has considerably increased and these researches now play an important role in elementary particle physics. Indeed several factors seem to attract attention to this field. Firstly, progress in experimental techniques has made feasible a number of difficult experiments, which were suggested long ago, but could not be realized in a full scale because of the low probabilities of the processes of interest and because of the difficulties associated with a high background level. Secondly, purely theoretical progress in quantum chromodynamics and the fundamental concept of confinement have turned the physics of soft processes and large distances into an exciting new subject. So far one could not determine with certainty what type of experiment would be crucial for solving the extremely important confinement problem, but it seems quite likely that the first task is to find a number of phenomenological characteristics of hadrons, such as magnetic moments, formfactors, polarizability, mixing angles of quark and gluon combinations in their wave functions, etc. The study of electromagnetic decays and of other photon-proton interactions supplies rich data for this purpose. Information on the distribution of various quark configurations in hadronic matter can be obtained because electromagnetic phenomena reflect the interaction of photons with electric charges of quark fields. Such electromagnetic processes are found to be simpler and they allow one to make a more complete theoretical interpretation, than it is in the case for purely hadronic interactions. Consequently, these processes constitute a testing ground for any theory describing the structure of strongly interacting particles.

There is a great progress in the measuring of radiative decays of many mesons (see [1], reviews [2–5] and some recent works [6–8]) and for radiative transitions of baryon isobars N^* and Δ [1, 9]. Electromagnetic properties of isobars are investigated now very carefully in the resonance photoproduction and electroproduction reactions in the experiments with the new high-current electron facilities (CEBAF, ELSA — see, for example, [9, 10]).

Many topics were proposed and discussed in connection with radiative decays of hyperons and first of all for the low-lying hyperon states presented in Fig. 1.

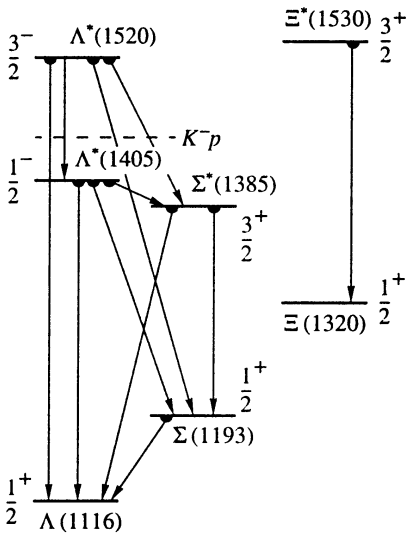

Fig. 1. Diagram of low-lying levels for hyperon resonances and of radiative transitions between these levels.

But the experimental situation here looks quite unsatisfactory. Up to now the only definite result was obtained for the well-known $\Sigma^0 \to \Lambda + \gamma$ decay: its width $\Gamma(\Sigma^0 \to \Lambda\gamma)$ was measured in two different experiments [11, 12] with compatible results (see Table 1). Both of them used the Coulomb production reaction $\Lambda + (\mathrm{Z}, \mathrm{A}) \to \Sigma^0 + (\mathrm{Z}, \mathrm{A})$ for these measurements.

The study of $\Lambda(1520) \to \Lambda + \gamma$ decay was performed also in two independent experiments in which $\Lambda(1520)$ hyperon was produced in s-channel resonance reaction $K^- + p \to \Lambda(1520) \to \Lambda + \gamma$ [13, 14]. But the results of these two measurements are in total disagreement (see Table 1). Thus the situation with this decay remains uncertain.

There were no direct observations of the decays $\Lambda(1405) \to \Lambda + \gamma; \Sigma^0 + \gamma$. Some information on these processes was obtained by an indirect method, in the study of radiative capture of kaons in K^--mesoatoms: $(K^- p)_{\mathrm{atom}} \to \Lambda + \gamma; \Sigma^0 + \gamma$ [15]. It was expected that properties of $K^- p$-atoms are strongly influenced by virtual $\Lambda(1405)$ hyperon, which is a resonant state lying just below $K^- p$ threshold (1432 MeV). From the radiative capture data, after some complicated and not straightforward theoretical calculations (see review [16]), the values of radiative decay widths $\Gamma(\Lambda(1405) \to \Lambda\gamma)$ and $\Gamma(\Lambda(1405) \to \Sigma^0\gamma)$ were obtained (see[17] and Table 1). But these results are not only model-dependent, but also not unique.

All the other radiative transitions, which are presented in Fig.1, up to now were not observed experimentally. Only some not very sensitive upper limits for their decay rates were obtained (Table 1).

Good possibilities to study some of these hyperon radiative decays are now opening up in the experiment E781 with a new high intensity and high energy hyperon beam of the Fermilab Tevatron [18]. The measurements of the cross sections for Coulomb production reactions $Y + (Z, A) \to Y^* + (Z, A)$ would be performed in the E781 experiment to determine the radiative widths $\Gamma(Y^* \to Y\gamma)$. The cross sections of these reactions are determined by the radiative widths $\Gamma(Y^* \to Y\gamma)$. These possibilities are discussed below in full detail.

Table 1. Theoretical predictions for radiative decays of hyperons and their comparison with experimental data (the radiative widths are in keV).

Model / Decay	SU3 symmetry	[22]	BAG [24, 26, 27]	NRQM [23, 24]	RQM [25]	Experiment
$\Gamma(\Delta^+ \to p\gamma)$	700	700	291–338			700 ± 50 [1]
$\Gamma(\Sigma^0 \to \Lambda\gamma)$	8.7	7.7	2.7–4.6	8.5–8.6	4.1 (6.7)	8.6 ± 1.4[11, 12]
$\Gamma(\Sigma(1385)^+ \to \Sigma^+\gamma)$	240	180	136–108	104–117		—
$\Gamma(\Sigma(1385)^- \to \Sigma^-\gamma)$	— (3.4)	0.5	1.5	2.4–2.1		< 24 [28]
$\Gamma(\Sigma(1385)^0 \to \Lambda\gamma)$	430	211–152	232–275	267 (161)		< 2000 [29]
$\Gamma(\Sigma(1385)^0 \to \Sigma^0\gamma)$	60	50	22-15	19–22	23 (14)	< 1750 [29]
$\Gamma(\Xi(1530)^0 \to \Xi^0\gamma)$	330	210	137–146	135		—
$\Gamma(\Xi(1530)^- \to \Xi^-\gamma)$	— (4.8)	0.8	1.9	2.6–2.8		—
$\Gamma(\Lambda(1405) \to \Lambda\gamma)$			17–75	143–200	118 (96)	27 ± 8 [17]
$\Gamma(\Lambda(1405) \to \Sigma^0\gamma)$			2.4–27	72–91	46 (53)	10 ± 4 or [17]
						23 ± 7 [17]
$\Gamma(\Lambda(1520) \to \Lambda\gamma)$			27–46	96–156	215 (48)	134 ± 23 [13]
						31 ± 11 [14]
$\Gamma(\Lambda(1520) \to \Sigma^0\gamma)$			17–102	55-74	293 (31)	47 ± 17 [14]

Notes:
1. SU(3) symmetry — phenomenological estimations in SU(3) limit (in brackets are the estimations for U-spin forbidden decays in the Lipkin's model [21]). The results are normalized on the experimental value of the width $\Gamma(\Delta^+ \to p + \gamma)_{\rm exp} = 700 \pm 50$keV. Normalization factor is ~ 1.3.
2. Phenomenoligal model with SU(3) breaking by moderately-strong hypercharge dependent interactions [22]. The results are normalized on the experimental value of the width $\Gamma(\Delta^+ \to p + \gamma)_{\rm exp}$.
3. BAG — predictions in MIT bag [24, 26] and chiral bag [27] models.
4. NRQM — predictions in nonrelativistic quark models of Isgur-Karl type.
5. RQM — predictions from potential quark model with relativistic corrections; in brackets are the results, obtained in nonrelativistic approximation.

1. Radiative decays ${}^4[10]_{\rm SU(3)} \to {}^2[8]_{\rm SU(3)} + \gamma$

The schemes of hyperons, which belong to the ground SU(3) multiplets ${}^4[10]_{\rm SU(3)}$ and ${}^2[8]_{\rm SU(3)}$ are presented in Fig.2. These hyperons form U-spin multiplets, which are also specified in this figure. In the limit of strict SU(3) symmetry, U-spin is conserved for all processes. In electromagnetic reactions U-spin value for photon is zero. Thus, only radiative transitions between the states with the same value of U-spin are allowed. For ${}^4[10]_{\rm SU(3)} \to {}^2[8]_{\rm SU(3)} + \gamma$ decays:

$$\left.\begin{array}{l} \text{a) } (U=\frac{1}{2}) \to (U=\frac{1}{2}) + \gamma \left\{\begin{array}{l}\Delta^+ \to p + \gamma \\ \Sigma^{*+} \to \Sigma^+ + \gamma\end{array}\right. \\ \text{b) } (U=1) \to (U=1) + \gamma \left\{\begin{array}{l}\Sigma^{*0} \to \frac{1}{2}(\Sigma^0 + \sqrt{3}\Lambda) + \gamma \\ \Xi^{*0} \to \Xi^0 + \gamma\end{array}\right. \end{array}\right\} \text{allowed decays;}$$

$$\text{c) } (U=\frac{3}{2}) \to (U=\frac{1}{2}) + \gamma \left\{\begin{array}{l}\Sigma^{*-} \to \Sigma^- + \gamma \\ \Xi^{*-} \to \Xi^- + \gamma\end{array}\right\} \text{forbidden decays (suppressed by } U\text{-spin conservation).}$$

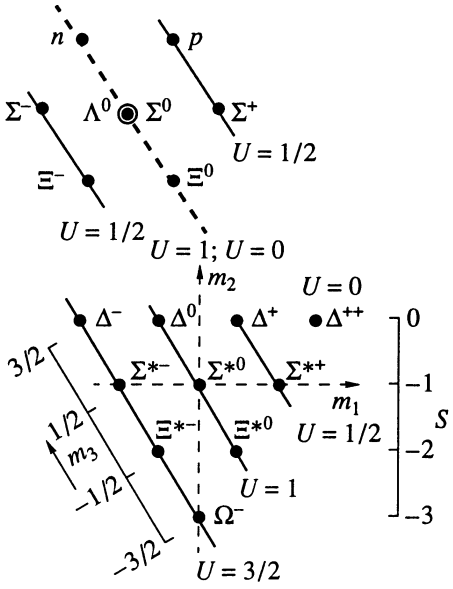

Fig. 2. Diagrams of the baryon octet and decuplet and structures of baryon multiplet in the U spin for these baryon families. For the baryon octet, the superpositions $|u_1>=|U=1;U_3=0>=|\frac{1}{2}(\Sigma^0+\sqrt{3}\Lambda)>$ and $|u_0>=|U=0>=|\frac{1}{2}(\sqrt{3}\Sigma^0-\Lambda)>$ are neutral states with definite U-spin values. The other notations are as follows: S is strangeness, $m_1=I_3$; $m_2=Y=B+S$; $m_3=U_3$.

The radiative decays $B^*(J^P{=}\frac{3}{2}^+)\to B(J^P{=}\frac{1}{2}^+)+\gamma$ are M1 or E2 electromagnetic transitions with the flip of spin of one of the quarks in B^*. The E2 amplitudes are very small and we shall consider only M1-decays. The radiative width of this decay has the form:

$$\Gamma(B^*\to B\gamma)=\frac{1}{2}\left|\frac{\mu(B^*B)}{\mu_N}\right|^2\frac{\alpha}{M_p^2}P_\gamma^3. \tag{1}$$

Here $\mu(B^*B)$ is transition magnetic moment of $B^*B\gamma$ vertex (it determines the amplitude of the process), P_γ is the photon momentum, M_p is the mass of the proton, $\alpha=e^2/4\pi\simeq 1/137$, μ_N is the nuclear magneton.

In SU(3) symmetry limit it is possible to establish connections between the values of transition magnetic moments of different ${}^4[10]_{\rm SU(3)}\to{}^2[8]_{\rm SU(3)}+\gamma$ decays [19]:

$$\mu(\Delta^+p)=\mu(\Delta^0n)=-\mu(\Sigma^{*+}\Sigma^+)=\mu(\Xi^{*0}\Xi^0)=2\mu(\Sigma^{*0}\Sigma^0)=-\frac{2}{\sqrt{3}}\mu(\Sigma^{*0}\Lambda) \tag{2}$$

and

$$\mu(\Sigma^{*-}\Sigma^-)=\mu(\Xi^{*-}\Xi^-)=0. \tag{3}$$

At the same time, by using SU(6) symmetry relations it is possible to find the value of $\mu(\Delta^+p)$ transition magnetic moment:

$$\mu(\Delta^+p)=\frac{2\sqrt{2}}{3}\mu_p\quad(\mu_p=2.79\mu_N). \tag{4}$$

Now all the radiative widths for decuplet-octet decays can be estimated with the help of (1)-(4). But the radiative width estimation for $\Delta(1238)$ isobar $\Gamma(\Delta^+\to p\gamma)|_{\rm SU(6)}\simeq$ 500keV obtained from (1) and (4) is on $\sim 30\%$ lower than the experimental value for this width ($\Gamma(\Delta^+\to p\gamma)_{\rm exp}=696\pm 46$keV[1]). Besides, the overlapping integral I for

the wave functions of octet and decuplet baryon states must be included as a multiplier in equation (1). This correction factor may additionally reduce the value for $\Gamma(\Delta^+ \to p\gamma)|_{\rm SU(6)}(I \leq 1)$. Thus, we do not use the value of $\mu(\Delta^+ p)$ from (4) in further calculations and instead of this, we evaluate all the transition magnetic moments in (2) and all the radiative widths for $B^*(J^P = 3/2^+) \to B(J^P = 1/2^+) + \gamma$ decays with normalization based on the experimental value of $\Gamma(\Delta^+ \to p\gamma)$. The results of this "normalized SU(3) approximation" are presented in the first column of Table 1 ("SU(3) symmetry"). These radiative widths lay $\sim 30\%$ higher than the values obtained in SU(6) approximation (4). It seems to us that such normalization can reduce the uncertainties connected with simple nonrelativistic equation (1) and, to some extent, take into account recoil corrections, effects of pion exchange currents, etc.

A simple estimation of possible SU(3) breaking and evaluation of the value of $\mu(\Sigma^{*-}\Sigma^-)$ and $\mu(\Xi^{*-}\Xi^-)$ transition magnetic moments was made by H. Lipkin [20] (see also [21]). The U-spin selection rule results (3) have a simple physical interpretation: $\Sigma^{*-}(dds)$ and $\Xi^{*-}(dss)$ hyperons contain only quarks with the same charges. Thus, in SU(3) limit their magnetic moments are also equal. The magnetic field of photon rotates all quark magnetic moments together by the same amount and the spin flip M1 transitions are forbidden. But SU(3) is broken because of the difference in the constituent quark masses of s- and u-, d-quarks ($m_s \simeq 510\,\mathrm{MeV}$; $m_{u,d} \simeq 310\,\mathrm{MeV}$), which leads to the difference in magnetic moments ($\mu_d = -0.972\mu_N$; $\mu_s = -0.613\mu_N$ — see PDG [1]). Thus, the decays $\Sigma^{*-} \to \Sigma^- + \gamma$ and $\Xi^{*-} \to \Xi^- + \gamma$ are not strictly forbidden, but only suppressed. Their transition magnetic moments are estimated in accordance with equation

$$\left|\frac{\mu(\Sigma^{*-}\Sigma^-)}{\mu(\Delta^+ p)}\right| = \left|\frac{\mu(\Xi^{*-}\Xi^-)}{\mu(\Delta^+ p)}\right| = \frac{1}{3}\left(1 - \frac{\mu_s}{\mu_d}\right) \simeq 0.123. \qquad (5)$$

The values of $\Gamma(\Sigma^{*-} \to \Sigma^-\gamma)$ and $\Gamma(\Xi^{*-} \to \Xi^-\gamma)$ obtained from (5) are also presented in the first column of Table 1, but in the brackets.

Another model for SU(3) and SU(6) breaking in the radiative decays of hyperons was developed in Ref [22], where it was assumed that this breaking is caused by moderate-strong interactions with transformation properties of superspinor of the second rank proportional to hypercharges of quarks. The phenomenological parameters of this model were obtained from the data on nucleon and hyperon magnetic moments. These parameters are used in the evaluation of transition magnetic moments for the decays $\Sigma^0 \to \Lambda + \gamma$ and ${}^4[10] \to {}^2[8] + \gamma$ (see Column 2 in Table 1, where again we use the normalization on the experimental value of $\Gamma(\Delta^+ \to p\gamma)$). It must be stressed that model [22] has a moderate precision for the description of baryon magnetic moments. But for the SU(3) forbidden decay $\Sigma^{*-} \to \Sigma^- + \gamma$ variations of the phenomenological parameters lead to a very large uncertainty (up to the factor of $2 \div 3$ in the radiative widths).

2. Results of theoretical calculations for hyperon radiative decay widths

All simple evaluations for hyperon radiative decay widths, presented in the previous section, give only approximate values of these widths in some naive phenomenological approach.

More sophisticated theoretical analysis was made in different variants of quark models, which are used for calculations of mass, wave function and decay widths of hyperon states (as well as other hadrons). Such calculations for hyperon properties were performed in the nonrelativistic QCD-inspired quark model of Isgur-Karl type (NRQM) [23, 24], in the quark model with relativistic corrections (RQM) [25], in different variations of bag model (MIT bag [24, 26], hiral bag [27]). Results of these calculations are summarized in Table 1 and are compared with the limited experimental data.

It is possible to conclude from this Table that for decuplet-octet transitions of S-state baryons, belonging to $[56]^{+}_{\mathrm{SU}(6)}$ representation, the results of different calculations are not in a very strong inconsistence among themselves due to a rather simple structure of their wave functions $|\Sigma(1385)\rangle \simeq \left|{}^4[10]_{\mathrm{SU}(3)}\right\rangle_{\frac{3}{2}^+}$, $|\Sigma\rangle \simeq \left|{}^2[8]_{\mathrm{SU}(3)}\right\rangle_{\frac{1}{2}^+}$, $|\Lambda\rangle \simeq \left|{}^2[8]_{\mathrm{SU}(3)}\right\rangle_{\frac{1}{2}^+}$ with only small mixing between SU(3) multiplets. But for P-state baryons belonging to $[70]^{-}_{\mathrm{SU}(6)}$ supermultiplet (for example, $\Lambda(1405)$ and $\Lambda(1520)$ hyperons) the situation is quite different. The spin-flavor mixing is very significant for these baryons and their wave functions in different models are drastically diverse. This leads to the discrepancy between the predicted radiative decay widths for different wave functions as large as a factor of 10-25. It is really a good point for future experiments to clarify the baryon structure.

3. Primakoff production processes for the measurements of radiative decay widths for hyperons

It is well known, that the coherent Coulomb production processes on the heavy nucleus ("Primakoff effect" [30, 31], see also [32, 33]) can be used for the measurements of radiative decay width for many hadronic states [11, 12, 34–36]. Such a possibility was discussed for the experiments with high energy charged hyperon beams [37–40] several times. The creation of high intensity hyperon beam at the Fermilab Tevatron with momentum $P^{-}_{\Sigma} = 650\,\mathrm{GeV}$ for the SELEX spectrometer [18] (experiment E781) gives a real possibility to realize this program in the nearest future, to measure radiative width of $\Sigma(1385)^{-} \to \Sigma^{-} + \gamma$ and may be $\Xi(1530)^{-} \to \Xi^{-} + \gamma$ (U-spin forbidden processes) and to compare them with the width of $\Sigma(1385)^{+} \to \Sigma^{+} + \gamma$ (U-spin allowed process).

The Coulomb production coherent reaction $h + (Z, A) \to a + (Z, A)$ (see diagram in Fig. 3) has very narrow transferred momentum distribution

$$\left.\frac{\mathrm{d}\sigma}{\mathrm{d}q^2}\right|_{\mathrm{Coulomb}} = 8\pi\alpha Z^2 \frac{2J_a+1}{2J_h+1}\Gamma(a \to h\gamma)\left(\frac{q^2 - q^2_{\mathrm{min}}}{q^4}\right)\left(\frac{M_a}{M_a^2 - M_h^2}\right)^3 |F_{\mathrm{em}}(q^2)|^2. \qquad (6)$$

Fig. 3. Diagram for the Coulomb process $h+(Z,A) \to a+(Z,A)$. The cross section for this reaction is proportional to the radiative width $\Gamma(a \to h+\gamma)$. The symbol V denotes vector meson ($ha\gamma$ vertex in the vector-dominance model).

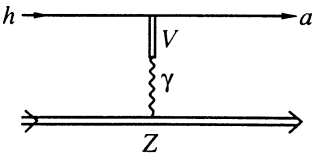

Here Z is the charge of nucleus, $\alpha \simeq 1/137$, $\Gamma(a \to h\gamma)$ is the radiative decay width of corresponding a decay, J_h, J_a and M_h, M_a are spins and masses of initial (h) and produced (a) hadrons, $F_{\rm em}(q^2)$ is the electromagnetic form-factor of nucleus, $q^2_{\rm min}$ is the square of minimal transferred 4-momentum, $q^2_{\rm min} = \left(M_a^2 - M_h^2\right)^2 / 4P_h^2$, P_h is the initial momentum. The differential cross-section of Coulomb production reaction increases very rapidly with the decrease of q^2 — up to the maximum value at $q_0^2 = 2q^2_{\rm min}$ (see Fig. 4). In the region of small q^2 ($< 0.005\,{\rm GeV}^2$) the Coulomb production mechanism dominates over the strongly produced coherent background (especially for very high initial momenta). The total cross section of the Coulomb production reaction has the form

$$\sigma_{\rm Coulomb} = 8\pi\alpha Z^2 \frac{2J_a+1}{2J_h+1}\Gamma(a \to h\gamma)\left(\frac{M_a}{M_a^2 - M_h^2}\right)^3 \int_{q^2_{\rm min}}^{q^2_{\rm max}} \frac{q^2 - q^2_{\rm min}}{q^4}\left|F_{\rm em}(q^2)\right|^2 {\rm d}q^2. \quad (7)$$

The value of $q^2_{\rm max}$ limits the region, where the Coulomb production mechanism dominates.

Fig. 4. Schematic behaviour of the differential cross section $[d\sigma/dt]_{Coul}$ for the Coulomb production process $h+(Z,A) \to a+(Z,A)$ (see the diagram in Fig.3). In this figure $|t| = q^2$ is the squared momentum transfer, and $|t_0| = 2|t_{min}|$ is the value of $|t|$ that corresponds to the maximum differential cross section $[d\sigma/dt]_{Coul}$. The maximum cross section grows with energy in proportion to E_h^2, while the position of the peak shifts towards lower $|t_0|$ values according to the E_h^{-2} law. The dash-dotted curve represents the background from the coherent strong interaction processes.

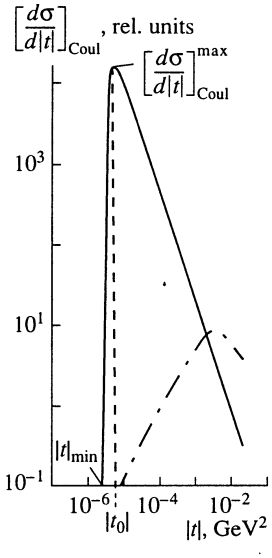

The electromagnetic formfactor of nucleus is parametrized in the form of

$$F_{\rm em}(q^2) = \exp(-q^2/b^2), \quad (8)$$

where $b^2 = 6/\langle r^2\rangle$ and RMS of the radius of nucleus is $\sqrt{\langle r^2\rangle} = 0.94A^{1/3}10^{-13}\,{\rm cm}$ (see, for example, [41]). With this formfactor

$$I = \int_{q^2_{\rm min}}^{q^2_{\rm max}} \frac{q^2 - q^2_{\rm min}}{q^4}\left|F_{\rm em}(q^2)\right|^2 {\rm d}q^2 \simeq \ln\frac{x_{\rm max}}{x_{\rm min}} - x_{\rm max} + \frac{x^2_{\rm max}}{4} - 1, \quad (9)$$

where $x^2 = q^2/a^2$, $a^2 = b^2/2$ and it was presumed that $x_{\min} \ll x_{\max}$, $x_{\max} < 1$. For lead nuclei $\sqrt{\langle r^2 \rangle} = 5.56{\cdot}10^{-13}\,\mathrm{cm}$, $b^2 = 0.0078\,\mathrm{GeV}^2$, $a^2 = 0.0039\,\mathrm{GeV}^2$, the value of I is

$$I = \ln \frac{q^2_{\max}}{q^2_{\min}} - 1.8. \tag{10}$$

For large enough P_h ($\ln(q^2_{\max}/q^2_{\min}) > 5 \div 6$) this result is not very sensitive to the parameterization of the formfactor $F_{\mathrm{em}}(q^2)$. For other parameterizations we obtain:

$$F_{\mathrm{em}}(q^2) = (1 - q^2/b^2); \qquad I = \ln \frac{q^2_{\max}}{q^2_{\min}} - 2.0, \tag{11}$$

$$F_{\mathrm{em}}(q^2) = 1/(1 + q^2/b^2)^2; \quad I = \ln \frac{q^2_{\max}}{q^2_{\min}} - 2.8, \tag{12}$$

$$F_{\mathrm{em}}(q^2) = 1; \qquad I = \ln \frac{q^2_{\max}}{q^2_{\min}} - 1.0. \tag{13}$$

Expressions (7) and (9) can be used for the estimations of the rate of events in the Primakoff production reactions for U-spin forbidden processes

$$\begin{array}{rcl} \Sigma^- + (\mathrm{Pb}) & \to & \Sigma(1385)^- + (\mathrm{Pb}), \\ & & \quad \hookrightarrow \Lambda\pi^- \\ & & \qquad \hookrightarrow p\pi^- \end{array} \tag{14}$$

$$\begin{array}{rcl} \Xi^- + (\mathrm{Pb}) & \to & \Xi(1530)^- + (\mathrm{Pb}) \\ & & \quad \hookrightarrow \Xi^-\pi^0 \\ & & \qquad \hookrightarrow \Lambda\pi^- \\ & & \qquad\quad \hookrightarrow p\pi^- \end{array} \tag{15}$$

and for U-allowed one

$$\begin{array}{rcl} \Sigma^+ + (\mathrm{Pb}) & \to & \Sigma(1385)^+ + (\mathrm{Pb}). \\ & & \quad \hookrightarrow \Lambda\pi^+ \\ & & \qquad \hookrightarrow p\pi^- \end{array} \tag{16}$$

Instead of using reaction (16) in the positive beam, may be, it is possible (and preferable) to work with antisigma $\overline{\Sigma^+}$ hyperons in the negative beam by studying the reaction

$$\begin{array}{rcl} \overline{\Sigma^+} + (\mathrm{Pb}) & \to & \overline{\Sigma(1385)^+} + (\mathrm{Pb}) \\ & & \quad \hookrightarrow \overline{\Lambda}\pi^- \\ & & \qquad \hookrightarrow \overline{p}\pi^+ \end{array} \tag{17}$$

to measure all processes with excited hyperon resonances simultaneously and to reduce possible systematics in the comparison of the results for forbidden and allowed reactions.[1] In the cross section estimations we use the expected values for radiative decay widths of

[1] Now the rate for $\overline{\Sigma^+}$ in the beam is not known and a possibility of studying reaction (17) is not clear.

hyperons from Table 1. The results of these measurements should give us a possibility to determine all the three radiative decay widths by a clean method, which is practically free from any model assumptions.

A serious problem for these measurements is an absolute normalization of the $\bar{\Sigma^+}$ and Σ^- hyperon fluxes in the measurement of Coulomb production cross sections for Σ^{*-} and $\bar{\Sigma^{*+}}$ excitation. To evaluate the SU(3) suppression of $\Sigma^{*-} \to \Sigma^-\gamma$ it is important to know the ratio of the fluxes $I(\bar{\Sigma^+}/I(\Sigma^-)$ in the negative hyperon beam. The monitoring of these fluxes can be performed with registration of hyperon decays $\Sigma^- \to \pi^- + n$ and $\bar{\Sigma^+} \to \bar{p}\pi^0$ ($\bar{\Sigma^+} \to \bar{n}\pi^-$ decay is impossible to separate from $\Sigma^- \to n\pi^-$). To test the Monte-Carlo simulation of efficiencies for the detection of these decays it is desirable to use the data for $\Sigma^+ \to p\pi^0$ and $\Sigma^+ \to n\pi^+$ decays in the run with a positive beam.

4. Trigger possibilities, efficiency and trigger rates

Data on the Primakoff production reactions (14), (16) and may be also (15), (17) would be obtained in the framework of the Fermilab experiment E781 on the SELEX facility [18], which must carry out a wide hyperon physics research program in the intense charged hyperon beams with momenta up to 650 GeV. The main part of this program is connected with high statistics study of the spectroscopy of charmed and strange-charmed baryons as well as weak decays of these particles. Besides, it is planned to study simultaneously electromagnetic properties of hyperons and mesons (their formfactors, polarizabilities), to search for the exotic states of different kinds, to study rare weak decays of hyperons and some other processes.

A general layout of the SELEX facility is presented in Fig.5. The apparatus includes the three-stage magnetic spectrometer with proportional and drift chambers, vertex microstrip detector, trigger hodoscopes, some additional microstrip detectors, RICH and TRD systems for particle identification, three photon spectrometers, neutron calorimeter.

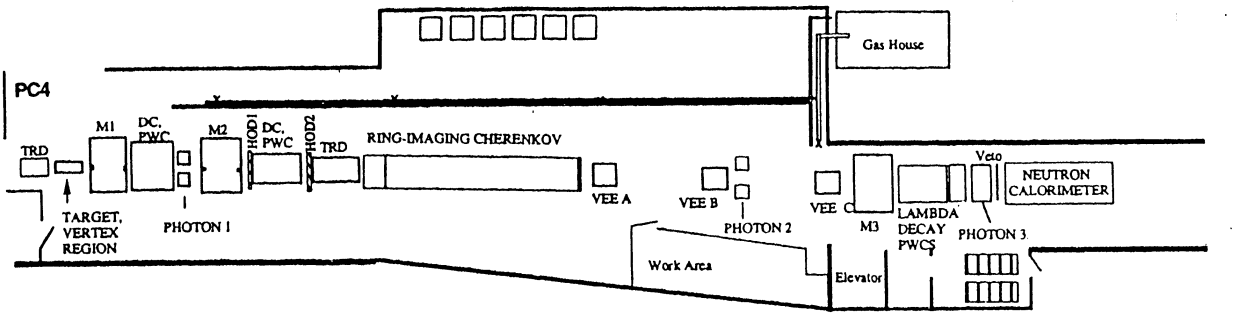

Fig. 5. The layout of the SELEX facility. $M_1 - M_2$ — magnetic spectrometers; DC — drift chambers; PC — proportional chambers, VEEA-VEEC — drift chamber clusters; Photon1-3 — multichannel lead glass γ-spectrometers; HOD1(H_1), HOD2(H_2) — trigger hodoscopes, TRD — transition radiation detectors.

It is clear from (14)–(17) for the Primakoff reactions under study, that trigger conditions for the separation of these processes must be as follows: a) registration of one secondary particle just after the Primakoff lead target; b) registration of three charged particles after the decay path ($\sim 10\,\mathrm{m}$) for secondary (cascade) Λ-hyperon decay. For a) a special Primakoff trigger processor should be used (to separate a secondary particle after the target with angles $\theta_X, \theta_Y > 0.1\,\mathrm{mrad}$ relative to the incident particle). For b) trigger hodoscopes H1 and H2 with multiplicity requirements $M_{\mathrm{H1}} = 3$ and $M_{\mathrm{H2}} = 3$ could be used.

Below we will consider a possibility of using the silicon option of special Primakoff trigger processor [43] in some detail.

The goal of this processor is to guarantee the absence of beam particle after the Primakoff target, but the proposed construction allows one to use it for charm targets as well. The processor consists of three planes (or stations) with 50 micron strips (see Fig.6). Sizes and positions of the planes correspond to the beam phase space. First two stations are placed upstream of the lead Primakoff target. It is required that exactly one cluster be present in these planes. Based on the centers of clusters, the position of hit in the third station, which is placed downstream of the Primakoff and charm targets, is predicted. A trigger signal is generated, if the prediction is in the limits of the third station, and there are no hits in 3 (5, 7, this number is programmable) adjacent strips centered around the predicted one. It is also possible to work out necessary solutions from the Primakoff processor under more complicated experimental conditions, when there are more than one cluster in the first two planes of this device.

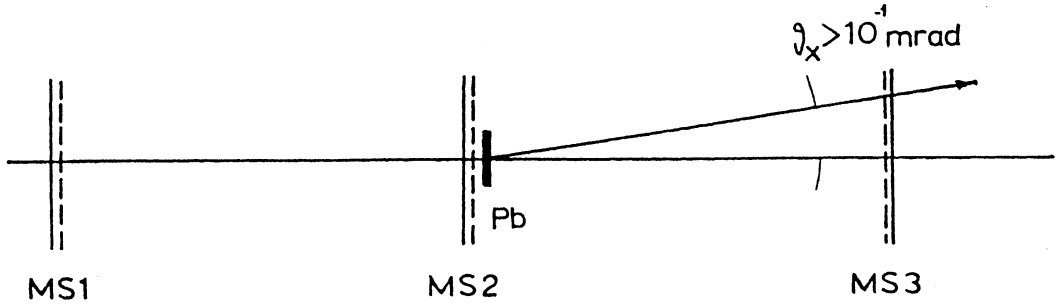

Fig. 6. The scheme of the Primakoff processor for the selection of the events with one particle after the target with anqles $\Theta_x, \Theta_y > 10^{-1}$ mrad (relative to the primary particle). MS 1-3 microstrip silicon detectors (with 50 μm strips); Pb — lead Primakoff target. This processor is now under development by PINP E781 group [43].

There are two projections of the microstrip planes in the Primakoff trigger processor. In any case, the computation is done in one projection and doesn't depend upon the other.

Preliminary position of the detectors and targets is summarized here[2]:

[2]Real geometry of the microstrip planes in the processor can be somewhat changed to compare with the above description. For example, the second plane in every projection can be placed immediately alter the lead Primakoff target. In any case the modification of the geometry does not significantly alter the results ol calculations.

	Z	X	Y
1st station	-310	3.7	0.0
2nd station	-150	4.8	0.0
Primakoff target	-100		
Charm target	0		
3rd station	70	6.2	0.0

Preliminary sizes of the stations and corresponding channel numbers are:

	$X \times Y$	X	Y
1st station	0.96x1.28	198	256
2nd station	1.28x1.44	256	288
3rd station	1.92x1.92	384	384

These sizes are capable of covering beam phase space (as it is currently defined in SELEX Monte-Carlo program GE781 version v2.01 for Ξ^--beam particles) completely.

Cut-off angles for different targets for 3, 5, 7 no-hit strips are:

	Primakoff target	Charm target
3 strips	0.044 mrad	0.107 mrad
5 strips	0.073 mrad	0.179 mrad
7 strips	0.103 mrad	0.250 mrad

The pion polarizability measurement puts a constraint on a cut-off angle: it should be no more than about 0.1 mrad, when viewed from the Primakoff target. It means that no more than 7 no-hit strips may be used in the third station. At the same time beam particles should be suppressed by a factor of about 100. If only one projection is used, possible numbers of no-hit strips are 5 and 7. Two projections allow for more flexibility, as one can make AND or OR of these two independent projections. As there are a lot of options, calculations were made just for two of them: 5 no-hit strips in case of one projection; 3 no-hit strips in each of two projections with subsequent AND. We will designate these options as 5 and 3×3.

Calculations were performed to estimate the Primakoff trigger processor efficiency for the following processes:

1. non-interacting beam particles;
2. $\Xi^- \to \Lambda\pi^-$ decays;
3. Primakoff production of $\Sigma(1385)^- \to \Lambda\pi^-$ (by Σ^- hyperons of the beam);
4. Primakoff production of $\Xi(1530)^- \to \Xi^-\pi^0$ (by Ξ^- hyperons of the beam);
5. diffractive production of $Y(ddss\bar{s})^- \to \Xi^- K^0_S$ [44] (by Σ^- hyperons of the beam).

Calculations were performed with the modified GE781 v2.01 program. It was assumed that alignment of microstrips was known and stable. Also, there were no hadron interactions, which had been taken into account in the simulation procedure. Thus, the results of beam particle suppression do not include elastic scattering and represent only geometrical features of the Primakoff trigger processor. The production of two-strip cluster by one charged particle was not taken into account. Decays of Λ were fixed to be to $p\pi^-$ only, so one must correct appropriate values for this branching.

4.1. Non-interacting beam particles

The efficiency was calculated for the beam Ξ^- particles, which have not decayed upstream with respect to the third station. Elastic scattering was not taken into account, so the numbers below reflect geometrical capabilities of the proposed processor:

Option	5	3×3
Efficiency	0.0	0.0048

As efficiency values are small, beam suppression will be determined by the elastic scattering (on the level of 10^{-3}), or by inefficiency of the third station.

4.2. $\Xi^- \to \Lambda\pi^-$ decays

In this decay the root mean square of the angle of π^- with respect to Ξ^- in one projection is 1.0 mrad. Thus if Ξ^- decay has taken place somewhere between the first and third stations, it usually gives a trigger signal in the processor. As Ξ^- decay suppression due to the Primakoff trigger processor correlates with suppression due to other trigger requirements, the efficiency was calculated: a) for all Ξ^- beam particles existing at the end of hyperon magnet; b) for Ξ^- beam particles decaying between the first and third stations; c) for Ξ^-, which give three digitizations in hodoscopes H1 and H2. The results are summarized here:

Option	5	3×3
Efficiency a)	0.12	0.12
Efficiency b)	0.81	0.80
Efficiency c)	0.45	0.43

4.3. Primakoff production of $\Sigma(1385)^- \to \Lambda\pi^-$

In this decay the root mean square of the angle of π^- with respect to beam in one projection is 1.4 mrad. Thus, the efficiency for registration of this process with the Primakoff trigger processor is good for both the Primakoff and charm targets

Option	5	3×3
Primakoff target	0.94	0.94
Charm target	0.90	0.88

4.4. Primakoff production of $\Xi(1530)^- \to \Xi^-\pi^0$

In this decay the root mean square of the angle of Ξ^- with respect to beam in one projection is 0.155 mrad. The efficiency is summarized here:

Option	5	3×3
Primakoff target	0.74	0.68
Charm target	0.39	0.37

4.5. Diffractive production of $Y(ddss\bar{s})^- \to \Xi^- K^0_S$

These estimations were performed in connection with the proposal for the search for exotic ($ddss\bar{s}$) hyperons (for the experiments on the search for strange cryptoexotic baryons with additional hidden strangeness, see [44]).

This process was simulated with P_T^2 slope $1000\,\mathrm{GeV}^2$, which is for sure greater, than it can be on Pb nucleus. This slope alone provides 0.04 mrad root mean square of the angle of Y^- with respect to beam. The efficiency of the Primakoff trigger processor strongly depends on the mass of the $Y^-(ddss\bar{s})$, and is summarized here (for charm targets):

Mass	Angle	Option	
(GeV)	(mrad)	5	3×3
1.85	0.19	0.49	0.44
1.95	0.42	0.78	0.72
2.05	0.57	0.82	0.80
2.15	0.77	0.86	0.84
2.25	0.94	0.90	0.86

4.6. Overall efficiency for the detection of $\Sigma(1385)^-$ and $\Xi(1530)^-$ Coulomb production reactions

Finally, for the Primakoff production of $\Sigma(1385)^-$ and $\Xi(1530)^-$, the geometrical efficiency for probable trigger requirements was estimated. The number of events generated and passed through different trigger requirements is presented in the following Table:

Process	$\Sigma(1385)^-$				$\Xi(1530)^-$			
Target	Primakoff		Charm		Primakoff		Charm	
Events and Eff.	N	Eff.	N	Eff.	N	Eff.	N	Eff.
Generated	852		847		871		852	
Primakoff (5)	796	0.934	757	0.894	636	0.730	324	0.380
$M_{\mathrm{IC}} = 1$	780		755		636		324	
$M_{\mathrm{H1}} = 3$	124		116		28		10	
$M_{\mathrm{H2}} = 3$	116	0.136	107	0.126	27	0.031	10	0.012
anti X at H2	109		105		27		10	
anti Y at H2	109	0.128	105	0.124	27	0.031	10	0.012
anti v≤1	101		101		27		10	
anti t≤1	94		95		27		10	
anti a≤2	74		77		22		9	
anti b≤2	66		66		16		7	
anti c≤2	64	0.075	66	0.078	16	0.018	6	0.007

Option with 5 no-hit strips was used for the Primakoff trigger processor. $M_{\mathrm{IC}} = 1$ designates the requirement of one charged particle in an interaction counter. $M_{\mathrm{H1}} = 3$ and $M_{\mathrm{H2}} = 3$ designate the requirement of 3 signals from hodoscopes H1 and H2. Anti X designates anticoincidence signals from margins of H2, which leave the remaining X

aperture of ± 35 cm. Anti Y designates anticoincidence from the special counters in the H2 region, which leave the remaining Y aperture of ± 10 cm. Anti x$\leq$n designates anticoincidence from square counters with size of 3 cm placed after each group of microstrip detectors: v — vertex; t — trigger; a — after magnet M1; b — before magnet M2; c — after magnet M2. A more detailed description of these requirements may be found in [44].

The results of these calculations show that for the Primakoff production of $\Sigma(1385)^-$ and $\Xi(1530)^-$ states one may use the trigger

$$T_{\rm Coulomb} = [\text{Primakoff trigger processor signal}] \times [M_{\rm H1} = 3] \times [M_{\rm H2} = 3].$$

The possibility to use additional anticoincidence signals described in [44] exists, in principle, but has not been realized now. It is possible to use these additional anticoincidences in future in case of necessity. The same is also true for the described in [44] diffractive production processes with appropriate changes on hodoscope multiplicity requirements.

The rate of this trigger is determined by the beam Ξ^- decays. If the flux of Ξ^- is $3{\cdot}10^3$ sec^{-1} (0.5% of full beam), then the corresponding trigger rate is about 10^2 per sec.

5. Expected statistics of the Coulomb production events and possible backgrounds

The results of calculations for the expected cross sections, the efficiency of registration and the number of events for the Primakoff production reactions (14), (15), (17) are presented in Table 2 (for somewhat idealized experimental conditions)

Table 2. Estimation of Primakoff production of hyperons and expected statistics for the optimal conditions of the experiments with hyperon beam.

Reaction	$\Gamma(Y^* \to Y\gamma)$ (keV)	Cross section $\sigma_{(\rm Pb)}$ (μb)	Hyperon flux (s^{-1})	BR	Eff.	Number of events (week^{-1})
(14)	2.3	410	$10^6\Sigma^-$	0.56	0.135	$2.3{\cdot}10^4$
(17)	110	$1.9{\cdot}10^4$	$0.4{\cdot}10^4\overline{\Sigma^+}$	0.56	0.135	450
(15)	2.7	310	$1{\cdot}10^4\Xi^-$	0.21	0.015	8

Notes:
1. Values of $\Gamma(Y^* \to Y\gamma)$ were chosen on the grounds of theoretical predictions in Table 1.
2. Thickness of lead Primakoff target is 3.5 g/cm^2, or $1{\cdot}10^{22}$ Pb/cm^2.
3. The "effective week" is equal to $7.5{\cdot}10^4$ s.
4. Efficiencies are taken from the data of section 5. For $\Xi(1530)^-$ registration additional factor 0.5 was assumed to account of π^0 detection.
5. BR is effective branching ratio for all secondary and cascade decays.

It must be borne in mind that the real circumstances of the E781 experiment turned out to be not so favorable as it was assumed before (significantly smaller intensity of the beam, other factors to reduce statistics.) Here we present some "realistic" estimates of the rates for processes (17), (18), based on the known conditions in the E781 run:

a) target 2mm Pb (2.3 g/cm^2, or $0.67 \cdot 10^{22} Pb$/cm^2);
b) beam $3.5 \cdot 10^5$ Σ^-/sec. or $7 \cdot 10^6$ Σ^-/spill;
c) 75 hours/week, or 4500 spills/week ($\sim 3 \cdot 10^{10}$ Σ^-/week)
d) efficiency (geom).BR=$0.135 \cdot 0.56 = 0.076$;
e) efficiency of reconstruction ~ 0.4;
f) lifetime factor =0.65

(in the works with the Primakoff processor the efficiency of this device must be taken into consideration — this value is unknown now).

For a positive beam of 450 GeV, the estimated beam flux is:

$$\begin{gathered} \text{protons} \sim 1.7 \cdot 10^6/\text{sec}; \\ \text{pions} \sim 0.3 \cdot 10^6/\text{sec}; \\ \Sigma^+ \sim 1.5 \cdot 10^4/\text{sec}. \end{gathered}$$

In the stand alone mode:

a) for negative beam — the expected number of Primakoff produced events with $\Sigma^*(1385)]^-$ is 1750 ev./week, or 250 ev./day;
b) for positive beam — the expected number of Primakoff produced $\Sigma^*(1385)]^+$ is 3500 ev./week, or 500 ev./day.

The use of the Primakoff processor in the trigger can reduced all these numbers ~ 2 times, but in any case, for ≤ 2 months of measurements, we would have enough statistics to determine $\Gamma[\Sigma^*(1385)^- \to \Sigma^- + \gamma$, $\Gamma[\Sigma^*(1385)^+ \to \Sigma^+ + \gamma]$ and their ratio with precision, which would be dependent only on systematics of the experiment.

It seems, at a glance, that the evaluation of a number of events in the Primakoff produced resonance peak of $\Sigma(1385)^- \to \Lambda\pi^-$ can be seriously affected by the background from $\Xi^- \to \Lambda\pi^-$ decay of beam particles, which has a rate of $\sim 0.5 \cdot 10^7$ event/week, i.e. *by* three orders of magnitude higher than the rate of $\Sigma(1385)^-$ production. But the measurement of the $\Lambda\pi^-$ production vertex will be made with $\sigma_Z = 0.4\,$cm precision[3]. At the same time, the effective decay path for beam Ξ^- in the Primakoff processor is about 300 cm. Thus, only about $0.8/300 \simeq 0.3\%$ of all the registered Ξ^- decays will be the real source of background. The expected precision in the effective mass $M(\Lambda\pi^-)$ measurement for Ξ^- decays is $\sigma_M \simeq 5 \div 10\,$MeV. Thus, the number of background Ξ^- decay events under $\Sigma(1385)^-$ peak will be on a percent level.

We have evaluated also the influence of the strong coherent production of $\Sigma(1385)^-$ and $\Xi(1530)^-$ on the Coulomb production of these states. From the extrapolation of the

[3] $\sigma_Z \simeq \sigma_{X,Y} / \langle\theta_{\pi^-}\rangle$. Precision of the track measurements in the beam and vertex microstrip detectors is $\sigma_{X,Y} \simeq 5\,\mu$m. Average deflection angle of π^- in $\Sigma(1385)^- \to \Lambda\pi^-$ decay is 1.4 mrad.

data of [21] to our energy and momentum transfer range, we conclude that the background due to strong coherent interactions must be no more than several percent.

To reduce the systematics in the absolute measurements of the cross sections for reactions (14)-(16) it is quite important to normalize Coulomb production of $\Sigma^*(1385)]^+$ with Coulomb production $p + Pb \to \Delta(1238)^+ + Pb$ (with the same trigger, by counting $\Delta^+ \to p + \pi^0$ with conversion of one photon in $e^+ e^-$ pair between interaction counter and H1 and with registration of the second photon in photon detectors, or with the trigger with 1 charged particle in the Primakoff processor and the hodoscopes H1, H2 and with some energy in Photon 3 detector). The radiative width of $\Delta(1238)^+ \to p + \gamma$ is a well known value $\Gamma(\Delta^+ \to p\gamma) = [700 \pm 50]$ KeV and may be used for normalization purposes. In the simultaneous measurements, even if the efficiency for π^0 registration is 0.01, the expected number of $\Delta(1238)^+$ Coulomb production events would be $4.75 \cdot 10^4$ ev./day.

To avoid the difficulties and additional systematics due to measurements with positive and negative hyperon beams under different conditions, it is possible and preferable to use also $\overline{\Sigma^+}$-hyperons in the negative beam with reaction $\overline{\Sigma^+} + Pb \to \overline{\Sigma(1385)^+} + Pb$.

In the same run with negative beam a lot of other interesting information about radiative transitions with hyperon resonances can be obtained (for example, for the decay $\Xi^*(1820)^- \to \Xi^- + \gamma$ and may be, for $\Xi^*(1530) \to \Xi^- + \gamma$).

6. The possibility to study radiative decays of heavier hyperons

Large sensitivity of the Primakoff exposition in E781 opens also a possibility to study radiative decays of some other (heavier) resonances of Σ^{*-} and Ξ^{*-} types. Let us consider here only one example — radiative decay of $\Xi(1820)^-$ hyperon. This state with $J^P = \frac{3}{2}^-$ belongs to SU(3) octet part of $[70]^-_{\mathrm{SU(6)}}$ supermultiplet. Thus, there is no U-spin suppression of $\Xi(1820)^- \to \Xi^- + \gamma$ radiative decay.

$\Xi(1820)^-$ hyperon is a very narrow state ($M = 1823.4 \pm 1.4\,\mathrm{MeV}$, $\Gamma = 24 \pm 5\,\mathrm{MeV}$) with the main decay channel $\Xi(1820)^- \to \Lambda + K^-$ with total branching $\mathrm{BR} \simeq 0.3 \times 0.64 \simeq 0.2$ (the same as for $\Xi(1530)^-$ — see Table 2), but with an order of magnitude larger efficiency of registration ($\epsilon \simeq 0.135$). The main factors which reduce this efficiency for $\Xi(1530)^-$ are cascade decays $\Xi^{*-} \to \Xi^- \to \Lambda$ on the limited decay path of the setup, and the necessity to registrate π^0 meson. Thus

$$[\mathrm{BR} \times \mathrm{Eff}]_{\Xi(1820)^-} \simeq 8[\mathrm{BR} \times \mathrm{Eff}]_{\Xi(1530)^-}. \tag{18}$$

Expression for the radiative widths of $\Xi(1530)^-$ and $\Xi(1820)^-$ is

$$\Gamma[Y^* \to Y\gamma] = |A(Y^* \to Y\gamma)|^2 \cdot P_\gamma^3 = \frac{1}{8}|A(Y^* \to Y\gamma)|^2 [\frac{M(Y^*)^2 - M(Y)^2}{M(Y^*)}]^3, \tag{19}$$

where $A(Y^* \to Y\gamma)$ is amplitude for radiative decay and P_γ is photon momentum.

Thus from (7) and (19) we obtain for Coulomb production of Y^* in Y^- — nucleus coherent interactions

$$\sigma(Y^*)_{\mathrm{Coulomb}} \simeq \mathrm{const} \frac{M(Y^*)^3}{(M(Y^*)^2 - M(Y)^2)^3} \Gamma(Y^* \to Y\gamma) = \mathrm{const}|A(Y^* \to Y\gamma)|^2 \tag{20}$$

(if $E_{\rm Y}$ is large enough and $\ln(q^2_{\rm max}/q^2_{\rm min}) \simeq$ const). Thus the cross sections do not depend upon kinematical factors ($M(Y^*)$ and $M(Y)$). In this case

$$\frac{\sigma(\Xi(1820)^-)_{\rm Coulomb}}{\sigma(\Xi(1530)^-)_{\rm Coulomb}} \simeq \left|\frac{A[\Xi(1820)^- \to \Xi^-\gamma]}{A[\Xi(1530)^- \to \Xi^-\gamma]}\right|^2 = P \tag{21}$$

and P can be a large factor ($\sim 10 \div 50$) because the radiative decay $\Xi(1820)^- \to \Xi^- + \gamma$ is not suppressed by U-spin conservation. Expected statistics of $\Xi(1820)^-$ in E781 run is $8 \times P$ times larger than that of $\Xi(1530)^-$, i.e. $\simeq 200\,$event/week.

7. Further study possibilities in E781 at Fermilab and in the SPHINX experiment at IHEP

It is very important to study radiative decays of $\Lambda(1405)$ and $\Lambda(1520)$ hyperons, for which theoretical predictions of different models are in disagreement by a factor of 10-25. There is a possibility to carry out the search for these radiative decays in the processes of diffractive production of hyperons like

$$\begin{array}{rcl} \Sigma^- + ({\rm N}) & \to & \Lambda^*\pi^- + ({\rm N}) \\ & & \quad \hookrightarrow \Lambda\gamma;\, \Sigma^0\gamma \end{array} \tag{22}$$

or

$$\begin{array}{rcl} p + ({\rm N}) & \to & \Lambda^* K^+ + ({\rm N}). \\ & & \quad \hookrightarrow \Lambda\gamma;\, \Sigma^0\gamma \end{array} \tag{23}$$

This possibility is now under study in the SELEX (reaction (22)) and the SPHINX (reaction (23)) experiments.

For a general description of the radiative decays of hyperon resonances see also [46].

References

[1] L.Montanet et al. (PDG)//Phys. Rev., 1994, v.50D, p.1173.

[2] H.Kolanoski//Springer Tracts Mod. Phys., 1984, v.105.

[3] P.J.O'Donnel//Rev. Mod. Phys., 1981, v.53, p.673.

[4] L.G.Landsberg//Phys. Reports, 1985, v.301, p.1280.
L.G.Landsberg//UFN, 1992, v.162, p.3.

[5] M.Zielinski//Acta Physica Polonica, 1987, v.18B, p.455.

[6] D.Alde et al. // Phys.Lett., 1994, v.340B, p.122.

[7] D.V.Amelin et al.//Z. Phys., 1995, v.66C, p.71.

[8] S.V.Donskov et al.//Proc "Hadron-93", Como, June 21-25, 1993, Nuovo Cim., 1994, v.107A, p.1799.

[9] V.D.Burkett//Intern. Jour. of Modern Phys., 1992, v.1E, p.421.

[10] C.N.Papanicolas, S.E.Williamson//Proc. "Hadron-91", 1991, p.145; S.A.Dytman//Ibid, p.155.

[11] F.Dydak et al.//Nucl. Phys., 1977, v.118B, p.1.

[12] P.C.Petersen et al.//Phys. Rev. Lett., 1986, v.57, p.949.

[13] T.S.Mast et al.//Phys. Rev. Lett., 1968, v.21, p.1715.

[14] R.Bertini et al.//10^{th} Int. Conf. PANIC, Heidelberg, Jule 30 - August 3, 1984, Conf. paper N 18;
see also R.Bertini //Nucl. Phys., 1987, v.279B, p.49.

[15] D.A.Whitehouse et al.//Phys. Rev. Lett., 1989, v.63, p.1352.

[16] J.Love.//Nuovo Cim., 1989, v.102A, p.167.

[17] H.Burkhard, J.Love.//Phys. Rev., 1991, v.440, p.607.

[18] R.Edelstein et al.//Fermilab proposal E781 (1987) (revised July 1993);
Workshop of E781 collaboration ("E781 Physics Days"), August 18-19, 1993, Internal Note 639.

[19] M.A.B.Bey et al.//Phys. Rev. Lett., 1964, v.13, p.514.

[20] H.J.Lipkin.//Phys. Rev., 1973, v.7D, p.846;
H.J.Lipkin, M.A.Moinester.//Phys. Lett., 1992, v.287B, p.179.

[21] A.V.Vanyashin et al.//Yad. Fiz., 1981, v.34, p.158 (Sov. J. Nucl. Phys., 1981, v.34, p.90).

[22] A.I.Ahiezer, M.P.Recalo.//Electrodynamics of hadrons, Kiev, "Naukova dumka", 1977;
A.I.Ahiezer, M.P.Recalo.//Pis'ma JETP, 1965, v.1, p.47.

[23] J.I.Darevich et al.//Phys. Rev., 1983, v.28D, p.1125.

[24] E.Kaxiras et al.//Phys. Rev., 1985, v.32D, p.695.

[25] M.Warns et al.//Phys. Lett., 1991, v.258B, p.431.

[26] R.H.Hackman et al.//Phys. Rev., 1978, v.18D, p.2537.

[27] Y.Umino, F.Myhrer.//Phys. Rev., 1989, v.39D, p.3391;
Y.Umino, F. Myhrer.//Nucl. Phys., 1991, v.529A, p.713.

[28] E.Arik et al.//Phys. Rev. Lett., 1977, v.38, p.1000.

[29] J.Colas et al.//Nucl. Phys., 1975, v.91B, p.253.

[30] H.Primakoff.//Phys. Rev., 1951, v.81, p.899.

[31] I.Ya.Pomeranchuk, I.M. Shmushkevich.//Nulcl. Phys., 1961, v.23, p.452.

[32] A.Halprin, C.M.Andersen, H.Primakoff.//Phys. Rev., 1966, v.152, p.1295;
J.Dreitlen, H.Primakoff.//Phys. Rev., 1962, v.125, p.1671.

[33] G.Fäldt et al.//Nucl. Phys., 1972, v.41B, p.125; v.43B, p.591.

[34] T.Jansen et al.//Phys. Rev., 1983, v.27D, p.26;
J.Huston et al.//Phys. Rev., 1986, v.33D, p.3199.

[35] S.Cihangir et al.//Phys. Lett., 1982, v.117B, p.119; Ibid, p.123;
Phys. Rev. Lett., 1983, v.51, p.1.

[36] B.Collick et al.//Phys. Rev. Lett., 1984, v.53, p.2374.

[37] M.V.Hynes.//Phys. in LAMPF II, LA-9798-P, p.333, Los-Alamos, 1984.

[38] V.I.Garkusha et al.//Preprint IHEP 90-81, Protvino, 1990;
L.G.Landsberg.//Proc. of Reinfels Workshop on the Hadron Mass Spectrum. St. Goar, Germany, September 3-6, 1990 (Ed. E. Klempt, K. Peters); Nucl. Phys. (Pros. Suppl.), 1991, v.211B, p

[39] L.G.Landsberg.//Proc. of Workshop "UNK-600", IHEP, Protvino, November 23-24, 1993, Protvino, 1994, p.27.

[40] M.Moinester.//Preprint TRI-PP-91-49, TAUP-1882-91, Invited Talk at 4^{th} Conf. on Intersections Between Particle and Nuclear Phys., May 24-29, Tuscon, Arisona.

[41] G.Fraunfelder, E. Hanly.//"Subatomic Physics".

[42] J.L.Langland.//Thesis, Univ. of Iowa, August, 1995.

[43] N.Terentiev.//Private communication.

[44] L.G.Landsberg, V.V.Molchanov.//Preprint IHEP 95-25, Protvino, 1995.

[45] D.V.Vavilov et al.//Yad. Fiz., 1994, v.57, p.241.

[46] L.G.Landsberg.//Yad.Fiz., 1996, v.59, p.2161.

Received June 9, 1997

Addendum

RADIATIVE DECAYS OF THE BARYON DECUPLET IN THE HEAVY BARYON CHIRAL PERTURBATION THEORY (HBChPT)

A new formalism of the heavy baryon chiral perturbation theory (HBChPT), which for the first time can consistently describe the dynamics of baryons near their mass-shell, was successfully developed in [A1].The lagrangian of HBChPT contains small expansion parameters connected with baryon masses and with chiral symmetry breaking scale. Perturbative calculations in this model probe the properties of QCD symmetries and their effects on the hadron processes.

The HBChPT approach was used for the analysis of the radiative decays from the baryon decuplet to the baryon octet ${}^4[10]_{SU(3)} \to^2 [8]_{SU(3)} + \gamma$ [A2,A3]. In these works the computation of the leading non-analytic SU(3) violation corrections induced at one-loop level were performed. This procedure gives possibility to estimate directly the probabilities for the SU(3) forbidden decays $\Sigma^*(1385)^- \to \Sigma^- + \gamma$ and $\Xi^*(1530)^- \to \Xi^- + \gamma$. For the calculation of radiative widths for SU(3) allowed branching ratios it is important to determine the values of two low energy constants. In [A2] it was done from the observed branching ratio for $\Delta^+ \to p + \gamma$ decay and from the present upper limit on $\Xi^{*0} \to \Xi^0 + \gamma$. The results of [A2] calculations are presented in Table 1A.

As it was claimed in the recent work [A3], their modified HBChPT calculations for the radiative decays of the baryon decuplet are more consistent and more precise than in [A2]. Parameter independent predictions for the SU(3) forbidden decays $\Sigma^{*-} \to \Sigma^- + \gamma$ and $\Xi^{*-} \to \Xi^- + \gamma$, which were obtained in [A3], are one order of magnitude larger than previous estimates in [A2] (see Table 1A). At the same time the authors of [A3] do not agree with the procedure of the determination of low energy constants, which was used in [A2]. It has been stated, that with available experimental data it is impossible now to fix these constants and to obtain the predictions for the radiative widths of the SU(3) allowed baryon decays for the decuplet.

It is instructive to compare the predictions in Table 1A with the same ones in Table 1 (see p.3). The large difference in predictions of different models and the new chiral model development in [A1-A3] make the measurements of radiative decays for the decuplet baryons (and especially of their SU(3) forbidden decay modes) one of the most important and exciting subjects in hadronic studying.

[A1] E.Jenkins and A.V.Manohar// Phys.Lett., 1991, v.B255, p.558.
[A2] M.N. Butler et al.//Nucl.Phys., 1993, v.B399, p.69; Phys.Lett., 1993, v.B304, p.353.
[A3] M.Napsuciale and J.L.Lucio M//Nucl.Phys., 1997, v.B494, p.260.

Table 1A. The predictions for the branching ratios and radiative decay widths for the ${}^4[10]_{\mathrm{SU(3)}} \to {}^2[8]_{\mathrm{SU(3)}} + \gamma$ decays in the framework of HBChPT.

Decay mode	[A2]		[A3]	
	BR	rad (keV)	BR	rad (keV)
$\Sigma^{*+} \to \Sigma^+ + \gamma$	$(2-6)\cdot 10^{-3}$	$70-215$		
$\Sigma^{*0} \to \Sigma^0 + \gamma$	$(4-10)\cdot 10^{-3}$	$140-360$		
$\Sigma^{*0} \to \Lambda + \gamma$	$(8-13)\cdot 10^{-3}$	$290-470$		
$\Xi^{*0} \to \Xi^0 + \gamma$	$(10-30)\cdot 10^{-3}$	$90-270$		
$\Sigma^{*-} \to \Sigma^- + \gamma$	$(4-6)\cdot 10^{-5}$	$1.6-2.4$	$2.4\cdot 10^{-4}$	9.5
$\Xi^{*-} \to \Xi^- + \gamma$	$(1-3)\cdot 10^{-4}$	$1-3$	$1.3\cdot 10^{-3}$	11.3

Л.Г.Ландсберг, В.В.Молчанов
Радиационные распады гиперонов.

Оригинал-макет подготовлен с помощью системы LaTeX.
Редактор Е.Н.Горина. Технический редактор Н.В.Орлова.

Подписано к печати 03.07.97. Формат 60 × 84/8. Офсетная печать.
Печ.л. 2.63. Уч.-изд.л. 2.02. Тираж 250. Заказ 1036. Индекс 3649.
ЛР №020498 17.04.97.

ГНЦ РФ Институт физики высоких энергий
142284, Протвино Московской обл.

Индекс 3649

П Р Е П Р И Н Т 97-42, И Ф В Э, 1997